

1 The association between rs6859 in *NECTIN2* gene and Alzheimer's disease is partly mediated by 2 pTau

3
4 Running Title: pTau connects *NECTIN2* and Alzheimer's disease

5
6 Aravind Lathika Rajendrakumar^{1*}, Konstantin G. Arbeev¹, Olivia Bagley¹, Anatoliy I. Yashin¹, Svetlana
7 Ukraintseva^{1*}

8
9 ¹*Biodemography of Aging Research Unit, Duke University, Social Science Research Institute, Durham, NC,*
10 *USA.*

11
12 Word count: 6,113

13 Number of tables and figures: 8

14 15 16 Abstract

17 18 Introduction

19 Emerging evidence suggests a connection between vulnerability to infections and Alzheimer's disease (AD).
20 The nectin cell adhesion molecule 2 (*NECTIN2*) gene coding for a membrane component of adherens junctions
21 is involved in response to infection, and its single nucleotide polymorphism (SNP) rs6859 was significantly
22 associated with AD risk in several human cohorts. It is unclear, however, how exactly rs6859 influences the
23 development of AD pathology. The aggregation of hyperphosphorylated tau protein (pTau) is a key
24 pathological feature of neurodegeneration in AD, which may be induced by infections, among other factors, and
25 potentially influenced by genes involved in both AD and vulnerability to infections, such as *NECTIN2*.

26 27 Materials and methods

28 We conducted a causal mediation analysis (CMA) on a sample of 708 participants in the Alzheimer's Disease
29 Neuroimaging Initiative (ADNI). The relationship between rs6859 and Alzheimer's disease (AD), with AD
30 (yes/no) as the outcome and pTau-181 levels in the cerebrospinal fluid (CSF) acting as a mediator in this
31 association, was assessed. Adjusted estimates from the probit and linear regression models were used in the
32 CMA model, where an additive model considered an increase in dosage of the rs6859 A allele (AD risk factor).

33 34 Results

35 The increase in dose of allele A of the SNP rs6859 resulted in about 0.144 increase per standard deviation (SD)
36 of pTau-181 (95% CI: 0.041, 0.248, $p < 0.01$). When included together in the probit model, the change in A
37 allele dose and each standard deviation change in pTau-181 predicted 6.84% and 9.79% higher probabilities for
38 AD, respectively. In the CMA, the proportion of the average mediated effect was 17.05% and was higher for
39 the risk allele homozygotes (AA), at 19.40% (95% CI: 6.20%, 43.00%, $p < 0.01$). The sensitivity analysis
40 confirmed the evidence of a robust mediation effect.

41 42 Conclusion

43 This study reported a new causal relationship between pTau-181 and AD. We found that the association
44 between rs6859 in the *NECTIN2* gene and AD is partly mediated by pTau-181 levels in CSF. The rest of this
45 association may be mediated by other factors. Further research, using other biomarkers, is needed to uncover
46 the remaining mechanisms of the association between the *NECTIN2* gene and AD.

47 48 Keywords

49
50 Alzheimer's Disease, *NECTIN2* gene, rs6859, pTau-181, causal mediation

54 1 Introduction

55 Alzheimer's disease (AD) is a debilitating neurodegenerative disorder that causes severe cognitive impairment
56 (Filho et al., 2017). Identification of biomarkers that accurately reflect pathological changes in the brain is
57 critical for AD prediction and treatment (Cox et al., 2022). Protein modification known as
58 hyperphosphorylation of Tau proteins (pTau) contributes to neurofibrillary tangles, a central feature of
59 Alzheimer's pathology (Drummond et al., 2020). The pTau concentrations were also linked to amyloid- β ,
60 another main AD biomarker, in a dose-response manner (Hirota et al., 2022). The utility of pTau as a sensitive
61 marker of AD has been well demonstrated (Moore, Hung, and Fortin 2023). Some studies also suggested that
62 the aggregation of pTau may be induced by infections, among other factors (Lee et al., 2022; Sathler et al.,
63 2022; Shen et al., 2022; Tang et al., 2022). The involvement of infections in AD is an emerging field of AD
64 research, and the literature on the factors that may influence both vulnerability to infections and
65 neurodegeneration is increasing (Yashin et al., 2018; Yong et al., 2021; Cairns, Itzhaki and Kaplan, 2022;
66 Mancuso et al., 2022; Nuovo et al., 2022; Piekut et al., 2022; Sathler et al., 2022; Tang et al., 2022;
67 Goldhardt et al., 2023; Ukraintseva et al., 2023; Popov et al., 2024). Nectin-2 (Nectin cell adhesion
68 molecule 2) is a membrane component of adherens junctions that serves as an entry point for certain
69 herpesviruses and may mediate response to the viral infection (Ogawa et al., 2022; Goldhardt et al., 2023).
70 The single nucleotide polymorphism (SNP) rs6859 of the *NECTIN2* gene was highly significantly associated
71 with AD risk in observational human data (Yashin et al., 2018; Mizutani et al., 2022). However, it is unclear
72 how exactly rs6859 facilitates the development of AD pathology. It is unlikely to be through the effects of
73 *APOE4* (located nearby, on the same chromosome 19), because rs6859 is not in the linkage disequilibrium with
74 *APOE4*. It is possible that the *NECTIN2* polymorphism contributes to AD through its involvement in
75 vulnerability to infections. Since pTau levels can be influenced by infections and related factors, we
76 hypothesized that they may also be influenced by the *NECTIN2* gene, involved in both AD and vulnerability to
77 infections, and could mediate the association of this gene with AD.

78
79 In this paper, we performed causal mediation analysis (CMA) to explore causal relationships among the rs6859
80 polymorphism in the *NECTIN2* gene, pTau, and AD using the Alzheimer's Disease Neuroimaging Initiative
81 (ADNI) data.

82 2 Materials and methods

83 2.1 Data

84
85 We used the UPENNBIOMK Master dataset publicly available from the ADNI consortium upon request
86 (adni.loni.usc.edu). ADNI is an ongoing research study envisaged under Michael W. Weiner with the original
87 aim of generating data from multiple biomarkers, along with clinical and other cognitive assessments, to learn
88 about mild cognitive impairment (MCI) and its conversion to full-blown AD in US older adults. The minimum
89 age of recruitment was 55 years, and the study tracks individuals with AD, cognitively normal, and milder
90 cognitive deficits across time (Weiner et al., 2017). The database currently contains comprehensive
91 measurements of various biomarkers, genetic variation, brain volume and structure, and cognitive status
92 (Weiner et al., 2010). The ADNI was conducted in 3 waves: ADNI 1, ADNI GO, ADNI 2, and ADNI 3. For
93 these phases, different genotyping platforms were used for genome-wide association studies (GWAS). These
94 were Illumina Human610-Quad BeadChip, Illumina HumanOmniExpress BeadChip, and Illumina Infinium
95 Global Screening Array v2 (GSA2), respectively, for ADNI waves 1-3. Biomarkers and cognitive
96 measurements were collected during the baseline and subsequent visits. The recorded number of visits ranged
97 from a single visit to a maximum of seven visits per participant. The ADNI data contain individual
98 measurements of pTau-181 levels in the cerebrospinal fluid (CSF) extracted using lumbar puncture and
99 quantified by the fully automated mid-region Roche Elecsys electrochemiluminescence immunoassays
100 platform. This pTau181 measure is considered a reference assay for comparing the performance of new pTau
101 epitopes in differentiating AD progression (Suárez-Calvet et al., 2020). We extracted the pTau-181
102 information with the corresponding subject ID (RID) and sample draw date and linked the files with age and
103 other demographical information from the demography file. The genotypes of SNP rs6859 were extracted from
104 the Plink binary files using the --recode command from the Plink 1.90 beta version (Purcell and Chang, 2023.;
105 Chang et al., 2015). The SNP information file was used to cross-check the genotype coding. We used the
106 ADNIMERGE file to determine the case and control status for AD.

107
108
109

110

111 2.2 The Causal Mediation Analysis (CMA)

112 In this analysis, we hypothesized that the effect of the *NECTIN2* polymorphism, represented by the SNP
113 rs6859, on AD is mediated through the pTau levels measured in the CSF. The CMA is a common method for
114 dissecting the total effect of treatment into direct and indirect effects (Nguyen, Schmid and Stuart, 2020). The
115 indirect effect is transmitted via a mediator to the outcome (Figure illustrating the CMA approach in the
116 supplement). The CMA will allow us to see if, and to what degree, the rs6859 could indirectly facilitate AD
117 occurrence through the pTau. In other words, what part of the association between rs6859 and AD could be
118 explained by the causal connection between pTau and AD.

119 Assessment of rs6859, pTau-181, and AD relationship

120 In this CMA, the relationship between rs6859 and AD, with AD (yes/no) as the outcome, and pTau-181 levels
121 (pg/mL) in the cerebrospinal fluid (CSF) acting as a mediator in this association, was assessed. The pTau-181
122 was a reasonable choice as a mediator variable for our CMA also because it allowed discrimination between
123 pathology-confirmed AD and other dementia subtypes (Grothe et al., 2021). Information on AD status (yes/no)
124 was an outcome. The control group included both cognitively normal individuals and subjects with dementia,
125 but not AD.

126 Statistical Analysis

127

128 We used R software version 4.0.0 (Vienna, Austria) to perform the analysis (R Core Team 2021). *ggplot2* and
129 *MuMin* packages were used for creating plots and regression model selection, respectively (Wickham, 2016;
130 Bartoň, 2013). Continuous variables with a normal distribution were summarized as mean \pm standard deviation
131 (SD) or median and interquartile range (IQR) for visually skewed distributions. For the causal mediation effects
132 analysis, an additive effect of the increasing dose of allele A of the SNP rs6859 was considered in the model.
133 For participants, different concentrations of pTau-181 were recorded during the same visit. To quantify the
134 variation for pTau-181, we calculated the overall median CV% change for the sample and the coefficient of
135 variation percentage (CV%) for repeat measures from the same day, along with their bootstrapped confidence
136 intervals (CI). For the corresponding measures, CV% was calculated by dividing the standard deviation by the
137 mean and then multiplying by 100. We did not employ a pass/fail criterion for the inclusion of values, as the
138 variations could be biologically relevant, and pruning the data could remove important information. To
139 understand these variations, boxplots were created for daily CV% variations across categorical variables. The
140 pTau-181 was summarized to a single reading per participant (median value) to obtain a more stable measure
141 and take advantage of multiple measures. pTau-181 was standardized, i.e., scaled and centred for regression and
142 mediation analyses. Age was computed from the final pTau-181 sample draw date and the birth date.

143

144 Separate regression models were fit to assess the association between pTau-181, rs6859, and AD. We
145 conducted a probit regression to examine the independent effect of rs6859, with the outcome adjusted for the
146 covariates based on an Akaike Information Criterion (AIC)-informed model (Cavanaugh and Neath, 2019).
147 Alternatively, a linear regression was run similarly for estimating the pTau-181 relationship with SNP rs6859.
148 The covariates included were age, sex, years of education, marriage status (divorced and never married vs.
149 married), smoking (yes/no), and alcohol use (yes/no). All possible combinations of covariates were run in the
150 model, and the model with the best AIC was selected. In the third step, the conditioned effects of rs6859 and
151 pTau-181 on the outcome variable were estimated in a probit regression model (Yin et al., 2016). Probit
152 regression model is a non-linear model for estimating the probability of being assigned to either of the
153 categories of a dichotomous outcome. It is similar to the logistic model except for the relationship with the link
154 function, which is based on a cumulative Gaussian distribution (Oyekale, 2021). The main advantage of the
155 probit model over the logistic model is that the former provides the probability of the event while treating the
156 covariate as a latent variable, while the odds ratio from the latter does not have the same interpretation (Yin et
157 al., 2016). The estimates from the probit regression model were presented as average marginal effects. Average
158 marginal estimates represent the average conditional probability associated with the variables represented on
159 the outcome scale (Williams, 2012). Lastly, the *mediate* function from the *mediation* package was used to
160 compute the mediation and proportion of mediated effects from the fitted models (Tingley et al., 2014).

161
162 We estimated the parameters by keeping the GG genotype of SNP rs6859 as the reference genotype while
163 considering the GA/AA genotype (carriers of allele A) at greater risk for AD. These were coded as 0, 1, and 2,
164 and the mediation effects were computed on allele (A) counts as in an additive model. We also computed the
165 effects for AA genotype individuals while choosing the GG genotype as the reference category (GG vs. AA).
166 The *mediation* package estimates an average effect for average causal mediation effects (ACME), average
167 direct effects (ADE), and an average for the proportion of the mediated effects by decomposing the pre-
168 computed SNP rs6859 and standardized pTau-181 effects on AD in the combined model estimation step. This
169 step was required to quantify how the association between rs6859 and AD is mediated by pTau-181. ACME
170 represents the indirect effect of the SNP rs6859 on AD routed through pTau. ADE is the effect of the SNP
171 rs6859 on AD conditioned on the pTau-181. Similarly, the total effect is the sum of the direct and indirect
172 effects of rs6859 on AD. The proportion of the mediated effects is a complementary parameter to the ACME,
173 which simply quantifies the proportion of the mediated effect. A two-tailed p-value less than 0.05 was
174 considered significant for the regression models and mediation effects. The confidence intervals were estimated
175 with 5000 bootstrapped iterations with the *boot* option from the *mediation* package to obtain percentile
176 confidence intervals. We conducted a sensitivity analysis using the ρ values (correlation between the residuals
177 derived from the rs6859-AD association and rs6859 plus pTau-181, including a model for AD) plotted against
178 ACME values with 5000 simulations using the *medsens* command from the same package to check the
179 robustness of the results to see if they follow the sequential ignorability assumption (Pearl 2014).

180

181 3 Results

182

183 3.1 Sample characteristics

184

185 All participants with complete covariate information in the database were included in the analysis. The final
186 sample contained a total of 708 participants (Supplementary Figure S1). The pTau-181 level had a skewed
187 distribution with a median value of 34.20 pg/mL. There was a large variation in pTau-181 between individuals
188 (range: 6.9-213.0 pg/mL). The participant characteristics and demographic data are shown in Table 1. There
189 were 181 AD cases, accounting for 25.56% of the total sample. The frequencies for cognitively normal
190 individuals and individuals with cognitive deficiencies other than AD were 131 and 396, respectively.
191 Participants were predominantly of the white race (94.06%) and males. Close to 95.90% of the participants had
192 a marriage history, and 32.76% reported having a history of smoking. The proportion of participants with
193 GA/AA genotypes of SNP rs6859 was 73.87%. For some participants, there were large pTau-181 variations as
194 measured by CV% statistics (Supplementary Figures S2-S3). For the sample pTau-181 (CV%), the median was
195 6.08 (95% CI: 4.81, 7.15). Regarding pTau-181 (daily CV%), the median value was 1.33 (95% CI: 0.56, 2.15).
196 When it comes to daily CV%, there was no notable difference for rs6859 polymorphisms. However, daily CV%
197 variations were larger for males, individuals of white race, married participants, and those with a history of
198 smoking and alcohol use (Supplementary Figure S4).

199 The boxplot in Figure 1A illustrates the pTau-181 distribution for males and females. Females had relatively
200 higher median pTau-181 levels compared to males (35.1 vs. 33.0). GA carriers constituted the highest number
201 (357, or 50.42%) among the SNP rs6859 genotypes. The pTau-181 variation by age for carriers (GA/AA) and
202 non-carriers (GG) of SNP rs6859 allele A are shown in Figure 1B. The Pearson correlation heatmap for all
203 continuous variables is shown in Figure 2. There were no notable, strong correlations observed among the
204 variables. SNP rs6859 was positively correlated with pTau-181, although this correlation was relatively modest.
205 The SNP had a weak correlation with age (0.014) and education (-0.042), respectively.

206

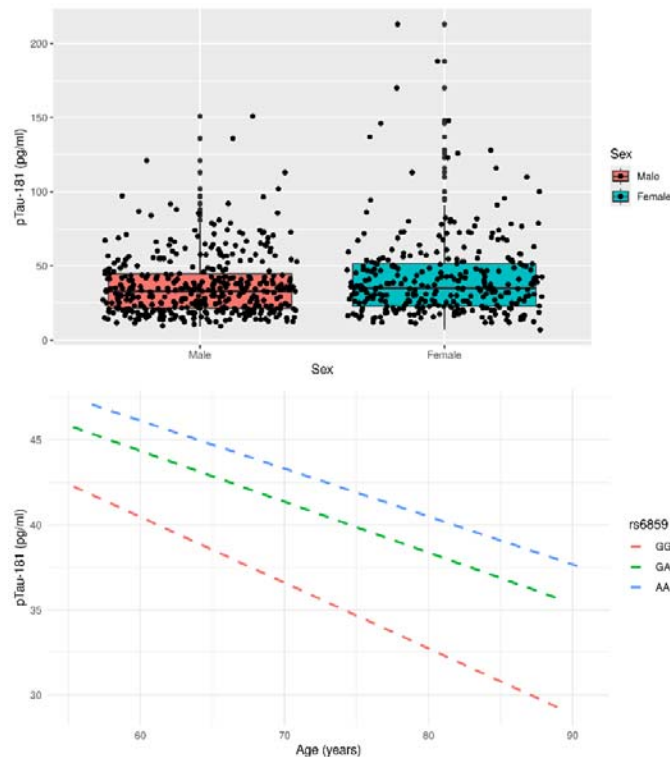
207 Table 1. Characteristics of participants in the study sample (n=708)

Parameter	Mean (Frequency)	SD	Range
Age (Years) #	74.19	7.19	55.33-90.79
Male (%)	399 (56.36%)		
Female (%)	309 (43.64%)		

Education (Years)	15.94	2.87	4-20
Marriage Status			
Ever	679 (95.90%)		
Never	28 (3.95%)		
Unknown	1 (0.14%)		
Race			
White	666 (94.06%)		
Other	42 (5.93%)		
Smoking (Ever)	232 (32.76%)		
Smoking (Never)	476 (67.24%)		
Alcohol (Ever)	29 (4.10%)		
Alcohol (Never)	679 (95.90%)		
pTau-181 (pg/mL) [#]	34.20 (95% CI: 32.0, 35.1)	26.17	6.9 - 213.0
pTau-181 (CV%) [#]	6.08 (95% CI: 4.81, 7.15)	17.15	0.0 - 77.6
pTau-181 (daily CV%) [#]	1.33 (95%: 0.56, 2.15)	8.37	0.00 - 82.68
SNP rs6859 (Genotype Frequencies)			
GG	185 (26.12%)		
GA	357 (50.42%)		
AA	166 (23.44%)		
SNP rs6859 (Allele Frequencies) ^{\$}			
G	51.34%		
A	48.66%		

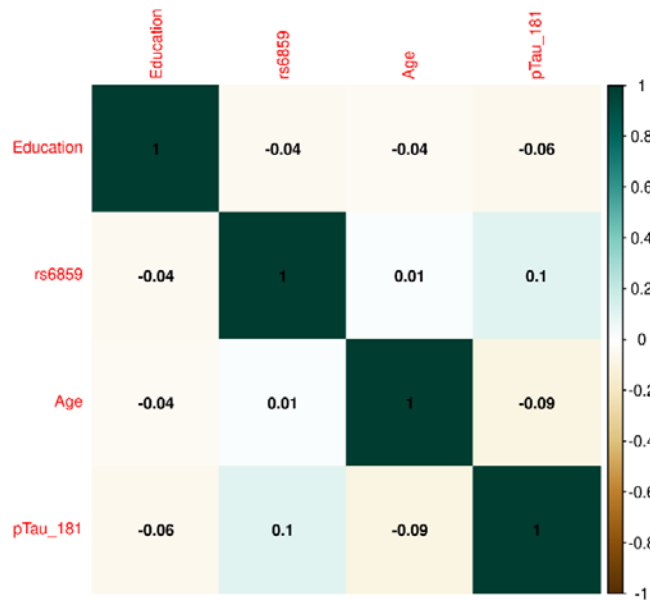
208 Note. Data are presented as mean \pm standard deviation (SD) or percentage (%) for continuous and categorical
 209 variables, respectively; [#] Age and pTau-181 are presented as median and IQR due to skewness of distributions.
 210 95% CI for median was calculated using the bootstrap method. ^{\$}Allele frequencies show the frequencies of SNP
 211 rs6859 alleles in the analysed sample.

212



213

214 Figure 1. (A) Distribution of pTau-181 by gender in the ADNI cohort (B) Variation of pTau-181 distribution by
 215 age and rs6859 genotype in the study sample



216

217

218 Figure 2. Correlation plot showing the relation for rs6859 with pTau-181 and other covariates in the ADNI
 219 dataset. Note. The size and colour of the circle indicate the strength and direction of the correlation between
 220 variables. The large dark blue dots show maximum correlation, i.e., correlation between the same variables in
 221 this case.

222

223 **3.2 The association of the SNP rs6859 with AD**

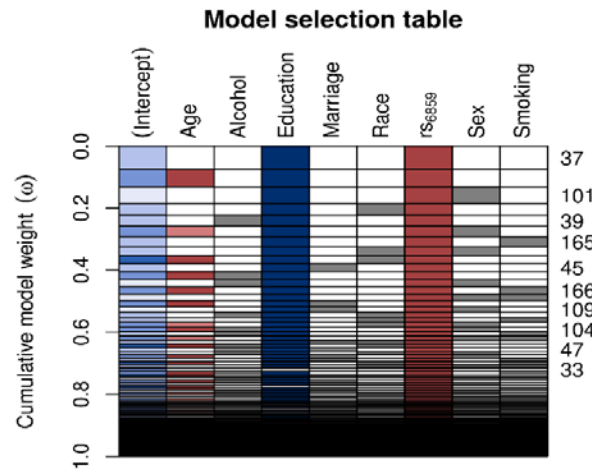
224 We found a statistically significant association between the SNP rs6859 and AD in the adjusted probit model.
225 We compared the model with a complete set of covariates to the best model, which is the model with the
226 minimal set of variables that best fits the data. The AIC - based model selection process is shown in Figure 3,
227 which illustrates the best model selection using the Akaike weights interpreted as the conditional probabilities
228 pertaining to the different combinations of the covariates (**Wagenmakers and Farrell 2004**). Of these, the best
229 model identified contained rs6859 and education (Supplementary Table S1). The AIC difference between the
230 models was close to 10 (Supplementary Table S2). The predicted z-score from the probit regression was 0.25
231 (95% CI: 0.11, 0.39, $p < 0.001$), which conveyed a higher probability of being classified as AD for the SNP
232 rs6859 additive model (A risk allele). Thus, the first requirement of the rs6859, which is that the former should
233 be significantly associated with both AD and pTau-181, is satisfied. The converted probit coefficients of
234 average marginal effects for the full model are presented in Supplementary Figure S5. The average marginal
235 effect estimates the percentage probability from the probit coefficients while keeping the effects from other
236 variables constant. As per the average marginal effects from the best model, there was a 7.9% higher percentage
237 probability of 0.079 (95% CI: 0.035, 0.124, $p < 0.001$) for AD associated with the genotype change from GG to
238 AA in the SNP rs6859. The only other important variable in this model was increasing years of education,
239 which showed a 1.3 decreased percentage probability of being classified as AD, -0.013 (95% CI: -0.024, -0.002,
240 $p < 0.05$).

241

242 **3.3 The association of SNP rs6859 with pTau-181**

243 For evaluating the model associations for SNP rs6859 with pTau-181, we ran linear regression models. The
244 model selection using Akaike weights is illustrated in Figure 4. SNP rs6859, age, race, and sex were selected as
245 the most significant predictors of pTau-181 in the best subset model. The AIC difference between the models
246 favored the model with a reduced set of covariates. The AIC for the different models is given in Supplementary
247 Table S3. In the age and sex-adjusted model, an increase in the dose of the A allele of the SNP rs6859 was
248 associated with an increase in the pTau-181 level. Respective coefficients and confidence limits for both models
249 are presented in Figure 5. Our analysis of the association between rs6859 and standardized pTau-181 levels was
250 statistically significant in the multivariate model and, therefore, independent of other risk factors, such as age
251 and smoking. The genotype change (GG to AA) of the rs6859 resulted in about a 0.144 increase per SD of
252 pTau-181 (95% CI: 0.041, 0.248, $p < 0.01$). Female participants were more likely to accumulate pTau-181 than
253 males. pTau-181 accumulation was comparatively higher in white individuals (0.277, 95% CI: -0.031, 0.586,
254 $p = 0.078$). However, the coefficient was not statistically significant. Surprisingly, a year of the increase in age
255 was associated with a reduction in pTau-181 (-0.011, 95% CI: -0.021, -0.001; $p < 0.05$). Therefore, we ran a
256 linear mixed model with a larger sample size (records = 2189, $n = 1249$) to confirm the association
257 (Supplementary Figure S6). Age, gender, education, and race were adjusted in the analysis. This dataset did not
258 include rs6859 information. Here, an increase in age predicted a 0.008 increase in pTau-181 (95% CI: 0.001,
259 0.015, $p < 0.05$). Our findings show that the diminished association for pTau-181 with age likely occurred as a
260 result of the smaller sample size arising from linking covariate information.

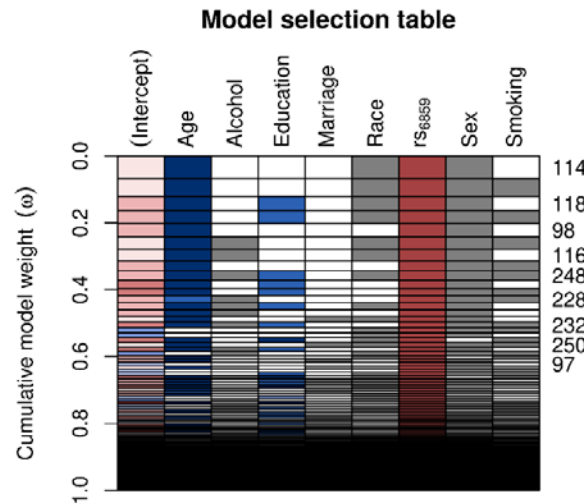
261



262

263 Figure 3. Model selection table depicting the AIC based variable selection process for the SNP rs6859 with AD.
 264 Note. The plot shows the model selection process in the automated model, ranked using AIC. Several models
 265 were run for different combinations of covariates (right-hand x-axis shown in each row), and a best subset
 266 model was selected. The models with a higher cumulative model weight indicate the best models. The best
 267 models are ranked in ascending order on the right-hand side of the plot. The row colours represent coefficient
 268 values, following a schema akin to a correlation heatmap, where blue signifies negative values and red denotes
 269 positive values. The model 37 carries the maximum weight of 0.075. The white row represents blank cells.

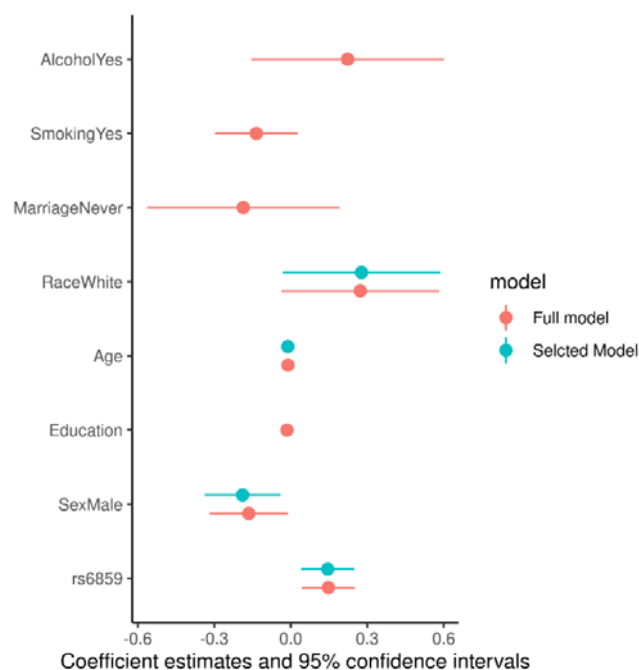
270



271

272 Figure 4. Model selection table depicting the AIC-based variable selection process for the rs6859 association
 273 with standardized pTau-181 (n=708). The plot shows the model selection process in the automated model,
 274 ranked using AIC. Several models were run for different combinations of covariates (right-hand x-axis shown
 275 in each row) and the best subset model was selected. The models with the higher cumulative model weights
 276 indicate the best model. The best models are ranked in ascending order on the right-hand side of the plot. Colors
 277 depict coefficient values, following a schema akin to a correlation heatmap, where blue signifies negative

278 values and red denotes positive values. Grey color is used to represent categorical variables. The model 114
279 carries a maximum weight of 0.066. The white row represents blank cells.
280
281

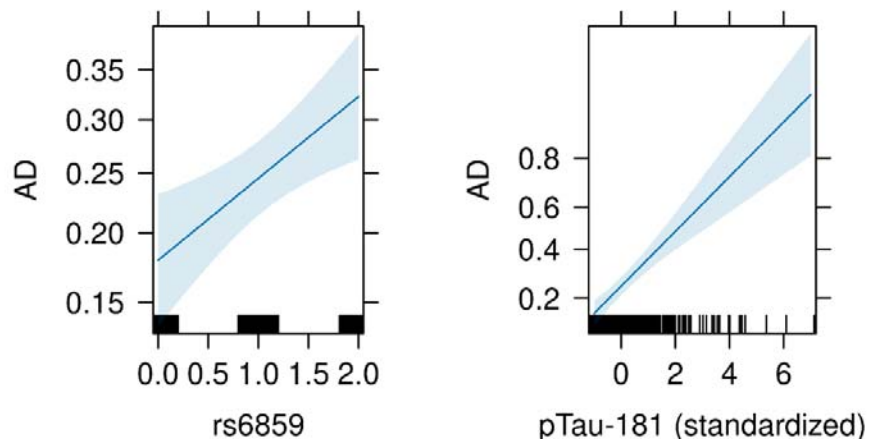


282
283 Figure 5. Coefficient estimates for the full and selected linear regression models for the pTau-181

284 3.4 Associations between the outcome, treatment variable, and dependent variable

285 For this analysis, we included the SNP rs6859 with standardized pTau-181 as covariates to generate estimates
286 to be used later in the causal mediation analysis. The predicted z-score from the probit model was significant
287 for both the rs6859 and mediator variables. The allele changes from G to A for the SNP rs6859 remained
288 similar to the previously computed estimate for AD (0.229, 95% CI: 0.081, 0.378, $p < 0.01$). For each standard
289 deviation change in pTau-181, there was a higher z-score, implying a higher probability of being classified as
290 AD (0.328, 95% CI: 0.225, 0.434, $p < 0.001$). Associated probabilities for SNP rs6859 and pTau-181 were
291 6.84% (95% CI: 2.49, 11.18, $p < 0.01$) and 9.79% (95% CI: 6.88%, 12.70%, $p < 0.001$), respectively. The
292 predicted effects from this model were visualized in the accompanying plot (Figure 6), showing an increase in
293 predicted risk associated with the unit change in rs6859 and pTau-181. As the model estimates were significant
294 for both rs6859 and pTau-181, the relationship is suggestive of a partial mediating effect as opposed to a full
295 mediating effect.

296
297



298

299 Figure 6. Conditioned effect plot illustrating the association of AD with rs6859 and pTau-181. Note. The plot
 300 was generated from a probit model with SNP rs6859 and pTau-181 as covariates. In Figure A, the dark blue line
 301 and surrounding light blue colour show the relationship and associated 95% confidence intervals for the
 302 genotype change and AD, respectively. In Figure B, the dark blue line shows the relationship and associated
 303 95% confidence intervals between pTau-181 and AD. The black colour lines in the x-axis for Figure A and
 304 Figure B correspond to observed values. The y-axis shows the estimates from the probit regression. A higher
 305 positive coefficient implies a higher AD probability.

306

307 3.5 Findings from the causal mediation analysis

308

309 The estimands from the CMA are reported in Table 2. The variation in the SNP rs6859 predates the pTau-181
 310 and AD. Therefore, SNP rs6859 variations could be considered a natural randomization and therefore do not
 311 have any direct influence on either the pTau-181 or AD. The estimates, as previously described, were generated
 312 from simulations, and the results indicate that the ACME, ADE, and total effect were significantly different
 313 from zero. Furthermore, the estimates could be interpreted as population averages for the specific genotypes
 314 (GG vs. AA) under a counterfactual scenario, i.e., the difference in average effects by holding the genotype
 315 effects for the AD, but switching between the values of pTau-181 observed with either of the genotypes
 316 (Tingley et al., 2014; Zhang et al., 2016). As hypothesized, both the ACME and ADE were higher for the AA
 317 compared to the GG genotype and were statistically significant. The ACME for both allele variations was 0.025
 318 and 0.033 ($p < 0.01$), respectively. Here, ACME represents the linear chain of effects of the specific genotype on
 319 AD probability, which is indirectly affected by pTau-181. It is to be noted that pTau-181 in turn is associated
 320 with the genotype in question. The ACME estimate informs us that there is statistically significant evidence for
 321 pTau-181 mediating the observed association of SNP rs6859 with AD. On top of that, the ADE was also
 322 significant and slightly higher for the AA genotype. Therefore, this suggests that the risk predicted for allele
 323 change in SNP rs6859 was partly mediated through pTau-181. The proportion of average-mediated effect was
 324 17.0% and was higher for the AA genotype (19.4%; 95% CI: 6.2%, 43.0%, $p < 0.01$). For the analysis between
 325 carriers and non-carriers shown in Supplementary Figure S7, the ACME was again statistically significant and
 326 high for the carrier group (0.024 vs. 0.018, $p < 0.01$). The corresponding proportions of the mediated effects were
 327 18.98% and 14.56%, respectively.

328

329 Table 2. Causal mediation analysis showing the estimate of the effect on the association between rs6859 and
 330 Alzheimer’s Disease mediated through pTau-181 (n=708)

331

Effect	Estimate	95% Lower CI	95% Upper CI	p
ACME (GG)	0.025	0.007	0.050	0.003**

ACME (AA)	0.033	0.009	0.060	0.003**
ADE (GG)	0.137	0.052	0.220	0.002**
ADE (AA)	0.145	0.055	0.230	0.00**
Total Effect	0.170	0.082	0.260	0.000***
Prop. Mediated (GG)	0.147	0.042	0.380	0.003**
Prop. Mediated (AA)	0.194	0.062	0.430	0.003**
ACME (average)	0.029	0.009	0.050	0.003**
ADE (average)	0.141	0.054	0.230	0.002**
Prop. Mediated (average)	0.170	0.052	0.410	0.003**

332
333 Note. The mediation estimates were jointly computed from separate regression model fits for AD and pTau as
334 outcomes. For the AD outcome, an independent effect of rs6958 conditioned for pTau was estimated with the
335 probit model. The independent effect of rs6958 on standardised pTau was calculated from a multivariate linear
336 regression model. **p<0.01; ***p<0.001. ACME (Average Causal Mediation Effect) indicates the part of the
337 rs6859 effect that is mediated by pTau-181. ADE (Average Direct Effect) refers to the part of the effect that is
338 independent of the pTau-181. Total Effect includes both the direct and indirect effects of rs6859. Proportion
339 Mediated is calculated as the ratio of the ACME to the total effect, representing the proportion of the effect that
340 passes through pTau-181 due to rs6859.
341

342 3.6 Sensitivity analysis for violation of the sequential ignorability assumption

343 A sensitivity analysis was carried out to check for the presence of unobserved confounders in the single
344 mediator model (as per **Cox et al. 2013**). The results are presented in Supplementary Figure S8. For this
345 purpose, a model correlation parameter ρ was calculated from the residuals of the models used to compute the
346 combined model. The values of the model parameter ρ were plotted on the x-axis against ACME on the y-axis.
347 The interpretation is based on the specific ρ values at which the ACME becomes zero or changes sign (positive
348 to negative). The corresponding ρ values were 0.2 and 0.3 for the former and latter, respectively. According to
349 the previous literature, the ρ values indicate that the estimands are relatively robust to the sequential ignorability
350 assumption, and there is evidence of a positive mediation effect (**Imai and Yamamoto, 2013; Zhang et al.,**
351 **2016**).

352 4. Discussion

353
354 Herein, we investigated a possible mechanistic link between the previously observed association between the
355 SNP rs6859 in the *NECTIN2* gene and AD, using pTau as a mediator of the rs6859 effect on AD. Tauopathies
356 are recognised players in neurologic disorders (**Hernández and Avila, 2007**). There is substantial evidence of
357 associations between pTau-181 state changes and AD-relevant markers, often decades before the development
358 of aggregated tau pathology in the brain (**Barthélemy et al., 2020**). Despite this, it is still not clear if pTau
359 build-up directly causes AD or if it is driven by alternative biological mechanisms (**Jack et al., 2018**). To our
360 knowledge, this is the first study to uncover a causal role for pTau-181 in AD from the association between
361 variation in the *NECTIN2* gene and AD using the CMA approach. This CMA revealed that 17.05% of the
362 rs6859 effect on AD is mediated through the pTau. Our results thus suggest that the accumulation of pTau is a
363 *partial cause* of AD, and other, including unknown, pathways likely contribute to AD too. The latter is rather
364 expected since AD is a heterogeneous complex health disorder and may include cases of different etiology.
365

366 Several ptau isoforms exist that could be utilized to study Alzheimer's disease (AD) pathology (Suárez-Calvet
367 *et al.*, 2020; Hirota *et al.*, 2022b; Salvadó *et al.*, 2024). Numerous studies have explored the utility of these
368 markers over the years, often yielding conflicting results (Hampel *et al.*, 2004; Vacchiano *et al.*, 2023;
369 Ingannato *et al.*, 2024; Salvadó *et al.*, 2024). Consequently, there is still debate regarding the best marker for
370 AD, and new candidates are continually being proposed (Suárez-Calvet *et al.*, 2020; Karikari *et al.*, 2021;
371 Salvadó *et al.*, 2024). Assessing the diversity of ptau isoforms in relation to AD pathology is challenging, as
372 these isoforms appear at different stages of AD and exhibit heterogeneous relationships with amyloid plaques
373 and neurofibrillary tangles (Wennström *et al.*, 2024). For instance, an earlier study comparing phosphorylation
374 at threonine 231 (p-tau231), threonine 181 (p-tau181), and serine 199 (p-tau199) in cerebrospinal fluid (CSF)
375 showed that ptau181 could classify AD with Lewy body dementia better than p-tau231, which differentiated
376 AD from frontotemporal dementia. However, from a clinical prediction viewpoint, these markers were only
377 useful as standalone markers (Hampel *et al.*, 2004).

378 In mouse models, these markers were shown to be associated with synaptic dysfunction mediated by amyloid- β ,
379 with ptau181 specifically indicating axonal dysfunction (Hirota *et al.*, 2022). Another study among Swedes
380 demonstrated that ptau217 better reflected amyloid pathology and neurodegeneration than ptau181 and could
381 more effectively classify AD from other neurodegenerative conditions (Janelidze *et al.*, 2020). Later, this
382 finding was validated using plasma samples.(Thijssen *et al.*, 2021). However, both ptau181 and ptau217 share
383 similar pathology and increase before tau accumulation in AD (Janelidze *et al.*, 2020; Horie *et al.*, 2021). A
384 Canadian study detected CSF-based ptau231 changes before other biomarkers in AD as a response to amyloid- β -
385 initiated pathology (Ashton *et al.*, 2022). Despite their classification ability, these markers do not directly
386 translate to sensing disease severity. For example, postmortem examinations of AD brains showed that ptau231
387 did not robustly indicate AD severity (Buerger *et al.*, 2002).

388 Thus, selecting the ideal ptau isoform is critical for addressing the temporality question and capturing early
389 onset and progression in AD. We chose ptau181 as a biomarker because it is considered a "classical AD
390 marker" and is the only ptau isoform currently measured among ADNI CSF biomarkers (Zetterberg and
391 Blennow, 2021). Plasma ptau181 levels have been demonstrated to outperform the A β 42/A β 40 ratio, another
392 important AD biomarker.(Thijssen *et al.*, 2020). Importantly, plasma ptau181 levels can capture early dementia
393 and are elevated in *APOE4* carriers, showing its pathological involvement in AD (Ingannato *et al.*, 2024).
394 Ptau181 correlates with neurodegeneration and cognitive decline in AD.(Moscoso *et al.*, 2021). Ptau181 assays
395 have demonstrated reliable prediction of AD progression.(Janelidze *et al.*, 2023). Furthermore, CSF-based
396 ptau181 is not influenced by other neurological conditions, unlike its plasma counterpart (Vacchiano *et al.*,
397 2023), and captures clear AD signatures compared to other dementias.(Zetterberg, 2017). All this evidence
398 shows that ptau181 is indeed a robust and tested marker of AD pathology (Thijssen *et al.*, 2021; Yu *et al.*,
399 2023).

400 Salvadó *et al.* utilized a machine learning algorithm to create a biological staging model for AD using
401 information from several biomarkers to predict AD progression. Their final set of biomarkers, however, did not
402 include ptau181 and p-tau231, as their contribution to the model was marginal. Interestingly, the A β 42/40 ratio
403 and p-tau217 remained part of their list (Salvadó *et al.*, 2024). Therefore, more studies are required to validate
404 and mechanistically understand how these isoforms relate to AD. Future research could use some of the
405 markers from Salvadó *et al.*'s study as mediators to replicate our work. However, it is difficult to say at this
406 stage whether these associations would yield a stronger causal relationship.

407 Another important gap is the lack of information regarding the tau form that can be labelled as representing
408 potential "post-infectious dementia". We are unaware of any specific study conducted on this topic to date.
409 Based on current evidence, we believe that the effect of infections on AD is primarily through inflammation,
410 which promotes AD pathological features like A β and ptau production (Cairns, Itzhaki and Kaplan, 2022b;
411 Ganz, Fainstein and Ben-Hur, 2022). Therefore, we hypothesize that a ptau isoform that best correlates with
412 inflammation could be a suitable predictor.

413 It is important to emphasize that we selected pTau-181 as a candidate mediator of the effect of rs6859 in the
414 *NECTIN2* gene on AD because both pTau and the *NECTIN2* gene have been linked to AD, as well as to
415 infections, in the literature (Yashin *et al.*, 2018; Sathler *et al.*, 2022; Tang *et al.*, 2022). From our previous
416 works, we also showed that upon vaccination for pneumonia and flu, rs6859 A allele carriers experienced a

417 reduced risk for AD (Ukrainitseva et al., 2023). Additionally, carriers of the A allele were likely to experience
418 cognitive decline, albeit at different rates (Rajendrakumar et al., 2024). In our study, the presence of the AA
419 genotype of the SNP rs6859 was associated with an increased percentage probability for AD (by 7.9%)
420 compared to the GG genotype, which is in line with previous findings from other cohorts (Yashin et al., 2018;
421 Logue et al., 2011). The increased pTau-181 levels in carriers of the rs6859 A allele are, however, not yet well
422 understood. Our results do not exclude the possibility that this increase in pTau may reflect a higher
423 vulnerability to infections as another underlying cause of AD. One hypothetical explanation could be that the
424 variation in the *NECTIN2* gene might increase the host vulnerability to infections, e.g., herpesviruses, which in
425 turn may promote neural damage and pTau accumulation in the brain, contributing to neurodegeneration
426 (Cairns, Itzhaki, and Kaplan, 2022; Powell-Doherty et al., 2020; Ogawa et al., 2022; Liu et al., 2018;
427 Readhead et al., 2018; Goldhardt et al., 2023). This potential mechanism deserves further investigation.

428

429 One should note that the CMA is not the only way to uncover causal relationships from the observed
430 associations. Mendelian randomization (MR) is another common approach. We, however, preferred the CMA
431 for this study because it provided a more attractive option to test the putative causal pathways, given the
432 possible role of confounding associations with the observed findings for SNP rs6859 with pTau-181 and AD
433 (Sait et al., 2021). The CMA, at least in theory, is less stringent than the assumptions associated with MR
434 studies, which assume a much stricter instrument variable and an intermediate outcome pathway (Rijnhart et
435 al., 2021). The CMA with an ideal “treatment” should produce estimates similar to those in the MR (Carter et
436 al., 2021). Additional strengths of this study include the availability of longitudinal biomarker measurements in
437 the ADNI and the use of sensitivity analysis. An important limitation of this study is the incomplete data on
438 covariates for some ADNI participants, which led to a smaller sample size than initially expected. Other
439 limitations include the lack of supporting evidence for our findings, particularly regarding how the *NECTIN2*
440 SNP rs6859 affects the production, processing, and deposition of beta-amyloids, and its modulation of β -
441 secretase (BACE1) activity. Furthermore, the Nectin2 protein, the end product of this gene, is not measured in
442 ADNI. Measuring Nectin2 protein levels could provide additional downstream insights. To address these gaps,
443 we plan to conduct future studies examining the relationship between SNP rs6859, beta-amyloids, and
444 hippocampal volume to better understand *NECTIN2*'s impact on AD phenotypes.

445

446 In conclusion, this study revealed a new causal relationship between pTau-181 and AD that partly explains the
447 association of the rs6859 polymorphism in the *NECTIN2* gene with Alzheimer's disease. Our findings in ADNI
448 data further strengthen the evidence of the association between rs6859 and AD, previously reported in GWAS
449 of other human cohorts (Yashin et al., 2018; Logue et al., 2011; Xiao et al., 2022), and provide a plausible
450 pathway linking the *Nectin2* polymorphism with AD. Predictably, the association between rs6859 and AD was
451 only partly mediated by pTau. The rest of the effect may be mediated through other, yet unknown, factors.
452 Further research is needed to uncover the remaining mechanisms connecting the variation in the *NECTIN2* gene
453 with AD.

454

455 **Data availability statement**

456

457 The data used in this article is publicly accessible through the ADNI website (<http://adni.loni.usc.edu>).

458

459 **Ethics statement**

460 The samples were collected with the written informed consent of all participants. Informed consent was
461 obtained from all subjects and/or their legal guardian(s). ADNI studies follow Good Clinical Practices
462 guidelines, the declaration of Helsinki and United States regulations (U.S. 21 CFR Part 50 and part 56). ADNI
463 studies were approved by all the respective Institutional Review Boards of academic institutions involved in the
464 consortium. For our specific study, we received approval from the Duke University Health System Institutional
465 Review Board under the Protocol IDs Pro00109279 and Pro00105389.

466

467 **Author Contributions**

468
469 S.U. and A.L.R. conceived the study. K.A., O.A.B., and A.L.R. were involved in data curation, analysis, and
470 data interpretation. S.U., K.A., and A.I.Y. provided guidance on data analysis and critically revised the
471 manuscript. All authors read and approved the final version of the manuscript.

472
473
474

Funding

475
476 Research reported in this publication was supported by the National Institute on Aging of the National Institutes
477 of Health under Award Numbers R01AG076019, R01AG070487. The content is solely the responsibility of the
478 authors and does not necessarily represent the official views of the National Institutes of Health.

479

Abbreviations

ACME	Average Causal Mediation Effects
AD	Alzheimer's Disease
ADE	Average Direct Effects
AIC	Akaike Information Criterion
A β	Amyloid β
BACE1	β -secretase
CV%	Coefficient of Variation Percentage
GWAS	Genome-wide association studies
HSV	Herpes Simplex Virus
IQR	Interquartile Range
pTau	Phosphorylated Tau
SD	Standard Deviation
SNP	Single Nucleotide Polymorphism
<i>NECTIN2</i>	Nectin Cell Adhesion Molecule 2 (gene)

481
482
483

Acknowledgements

484
485 The authors would like to thank the ADNI team. Data collection and sharing for this project was funded by the
486 Alzheimer's Disease Neuroimaging Initiative (ADNI) (National Institutes of Health Grant U01 AG024904) and
487 DOD ADNI (Department of Defense award number W81XWH-12-2-0012). ADNI is funded by the National
488 Institute on Aging, the National Institute of Biomedical Imaging and Bioengineering, and through generous
489 contributions from the following: AbbVie, Alzheimer's Association; Alzheimer's Drug Discovery Foundation;
490 Araclon Biotech; BioClinica, Inc.; Biogen; Bristol-Myers Squibb Company; CereSpir, Inc.; Cogstate; Eisai
491 Inc.; Elan Pharmaceuticals, Inc.; Eli Lilly and Company; EuroImmun; F. Hoffmann-La Roche Ltd and its
492 affiliated company Genentech, Inc.; Fujirebio; GE Healthcare; IXICO Ltd.; Janssen Alzheimer Immunotherapy
493 Research & Development, LLC.; Johnson & Johnson Pharmaceutical Research & Development LLC.;
494 Lumosity; Lundbeck; Merck & Co., Inc.; Meso Scale Diagnostics, LLC.; NeuroRx Research; Neurotrack
495 Technologies; Novartis Pharmaceuticals Corporation; Pfizer Inc.; Piramal Imaging; Servier; Takeda
496 Pharmaceutical Company; and Transition Therapeutics. The Canadian Institutes of Health Research is
497 providing funds to support ADNI clinical sites in Canada. Private sector contributions are facilitated by the
498 Foundation for the National Institutes of Health (www.fnih.org). The grantee organization is the Northern
499 California Institute for Research and Education, and the study is coordinated by the Alzheimer's Therapeutic
500 Research Institute at the University of Southern California. ADNI data are disseminated by the Laboratory for
501 Neuro Imaging at the University of Southern California.

502
503

Conflict of interest

504
505 The authors declare that they have no competing interests.

506
507
508

Supplementary material

509 **Supplementary Figure S1.** Study flow diagram showing the final sample selection in the ADNI cohort.
510 **Supplementary Figure S2.** Histogram showing daily Measurement variation for pTau-181 Indicated by CV%.
511 **Supplementary Figure S3.** Histogram Showing the overall sample variation for pTau-181 indicated by CV%.
512 **Supplementary Figure S4.** Boxplots showing daily CV% variation of pTau-181 for categorical variables.
513 **Supplementary Figure S5.** Average marginal estimates derived from the full variable probit regression model
514 for the prediction of AD. **Supplementary Figure S6.** Association of pTau-181 and age estimated from the
515 linear mixed models with sex, race, education, and smoking history as covariates assuming varying subject-
516 specific intercepts. **Supplementary Figure S7.** Contrasts in estimates of causal mediation analysis for SNP
517 rs6859 between carriers of GA/AA genotype and GG genotype with AD mediated through Ptau-181.
518 **Supplementary Figure S8.** Sensitivity analysis plot illustrating the model parameter ρ for checking the
519 sequential ignorability assumption. **Supplementary Table S1.** Estimates from the probit regression model for
520 SNP rs6859 association with AD from the selected AIC model. **Supplementary Table S2.** AIC for all the
521 different models explored for determining associations with the AD and SNP rs6859 using the probit model.
522 **Supplementary Table S3.** AIC for all the different models explored for determining associations with the
523 standardized Tau and SNP rs6859 using the linear regression model.

524

525 **References**

526

527 Ashton, N.J. *et al.* (2022) ‘Cerebrospinal fluid p-tau231 as an early indicator of emerging pathology in
528 Alzheimer’s disease’, *eBioMedicine*, 76, 103836. doi: 10.1016/j.ebiom.2022.103836

529 Barthélemy, N.R. *et al.* (2020) A soluble phosphorylated tau signature links tau, amyloid and the evolution of
530 stages of dominantly inherited Alzheimer’s disease, *Nat.Med*, 26, 398–407. doi.org/10.1038/s41591-020-0781-z

531 Bartoń, K. (2013) *MuMIn: Multi-model inference, R package version 1.10.0*. [https://cran.r-](https://cran.r-project.org/web/packages/MuMIn/index.html)
532 [project.org/web/packages/MuMIn/index.html](https://cran.r-project.org/web/packages/MuMIn/index.html) [Accessed April 4, 2023]

533 Buerger, K. *et al.* (2002) ‘Differential diagnosis of Alzheimer disease with cerebrospinal fluid levels of tau
534 protein phosphorylated at threonine 231’, *Arch Neurol*, 59(8), 1267–1272. doi: 10.1001/archneur.59.8.1267

535 Cairns, D.M., Itzhaki, R.F. and Kaplan, D.L. (2022) ‘Potential Involvement of Varicella Zoster Virus in
536 Alzheimer’s Disease via Reactivation of Quiescent Herpes Simplex Virus Type 1’, *J Alzheimer’s Dis*, 88(3),
537 1189–1200. doi.org/10.3233/jad-220287

538 Carter, A.R. *et al.* (2021) Mendelian randomisation for mediation analysis: current methods and challenges for
539 implementation, *Eur J Epidemiol*, 36, 465–478. doi.org/10.1007/S10654-021-00757-1

540 Cavanaugh, J.E. and Neath, A.A. (2019) The Akaike information criterion: Background, derivation, properties,
541 application, interpretation, and refinements, *WIREs Comput Stat*, 11: e1460. doi.org/10.1002/wics.1460

542 Chang, C.C. *et al.* (2015) Second-generation PLINK: Rising to the challenge of larger and richer datasets,
543 *GigaScience*, 4(1), s13742–015–0047–8. doi.org/10.1186/s13742-015-0047-8

544 Cox, M.F. *et al.* (2022) Friend or Foe? Defining the Role of Glutamate in Aging and Alzheimer’s Disease,
545 *Front Aging*, 3(929474). doi.org/10.3389/fragi.2022.929474

546 Cox, M.G. *et al.* (2013) Sensitivity Plots for Confounder Bias in the Single Mediator Model, *Eval Rev*, 37(5),
547 405- 431. doi.org/10.1177/0193841x14524576

548 Drummond, E. *et al.* (2020) Phosphorylated tau interactome in the human Alzheimer’s disease brain, *Brain*,
549 143(9), 2803–2817. doi.org/10.1093/brain/awaa223

550 Ganz, T., Fainstein, N. and Ben-Hur, T. (2022) ‘When the infectious environment meets the AD brain’, *Mol*
551 *Neurodegeneration*, 17(1),53. doi: 10.1186/s13024-022-00559-3

552 Goldhardt, O. *et al.* (2023) Herpes simplex virus alters Alzheimer’s disease biomarkers - A hypothesis paper,
553 *Alzheimer’s Dement*, 19(5), 2117–2134. doi.org/10.1002/alz.12834

- 554 Grothe, M.J. *et al.* (2021) Associations of Fully Automated CSF and Novel Plasma Biomarkers With Alzheimer
555 Disease Neuropathology at Autopsy, *Neurology*, 97(12), e1229–e1242.
556 doi.org/10.1212/wnl.00000000000012513
- 557 Hampel, H. *et al.* (2004) ‘Measurement of Phosphorylated Tau Epitopes in the Differential Diagnosis of
558 Alzheimer Disease: A Comparative Cerebrospinal Fluid Study’, *Arch Gen Psychiatry*, 61(1), 95–102. doi:
559 10.1001/archpsyc.61.1.95
- 560 Hernández, F. and Avila, J. (2007) Tauopathies, *Cell Mol Life Sci*, 64, 2219–2233. doi.org/10.1007/s00018-
561 007-7220-x
- 562 Hirota, Y. *et al.* (2022) Distinct brain pathologies associated with Alzheimer’s disease biomarker-related
563 phospho-tau 181 and phospho-tau 217 in App knock-in mouse models of amyloid- β amyloidosis, *Brain*
564 *commun*, 4(6): fcac286. doi.org/10.1093/braincomms/fcac286
- 565 Horie, K. *et al.* (2021) ‘CSF tau microtubule binding region identifies tau tangle and clinical stages of
566 Alzheimer’s disease’, *Brain*, 144(2), 515–527. doi: 10.1093/brain/awaa373
- 567 Imai, K. and Yamamoto, T. (2013) Identification and Sensitivity Analysis for Multiple Causal Mechanisms:
568 Revisiting Evidence from Framing Experiments, *Political Analysis*, 21, 141–171. doi.org/10.1093/pan/mps040
- 569 Ingannato, A. *et al.* (2024) ‘Plasma GFAP, NfL and pTau 181 detect preclinical stages of dementia’, *Front*
570 *Endocrinol (Lausanne)*, 15(1375302).
- 571 Jack, C.R. *et al.* (2018) NIA-AA Research Framework: Toward a biological definition of Alzheimer’s disease,
572 *Alzheimers Dement*, 14(4), 535–562. doi.org/10.1016/j.jalz.2018.02.018
- 573 Janelidze, S. *et al.* (2020) ‘Cerebrospinal fluid p-tau217 performs better than p-tau181 as a biomarker of
574 Alzheimer’s disease’, *Nat Commun*, 11(1) 1683. 10.1038/s41467-020-15436-0
- 575 Janelidze, S. *et al.* (2023) ‘Head-to-head comparison of 10 plasma phospho-tau assays in prodromal
576 Alzheimer’s disease’, *Brain*, 146(4), 1592–1601. doi: 10.1093/brain/awac333
- 577 Karikari, T.K. *et al.* (2021) ‘Head-to-head comparison of clinical performance of CSF phospho-tau T181 and
578 T217 biomarkers for Alzheimer’s disease diagnosis’, *Alzheimers Dement*, 17(5), 755–767. doi:
579 10.1002/alz.12236
- 580 Lee, S.E. *et al.* (2022) Zika virus infection accelerates Alzheimer’s disease phenotypes in brain organoids, *Cell*
581 *Death Discov*, 8, 153. doi.org/10.1038/s41420-022-00958-x
- 582 Liu, C. *et al.* (2018) Genome-Wide Association and Mechanistic Studies Indicate That Immune Response
583 Contributes to Alzheimer’s Disease Development, *Front Genet*, 9(410). doi.org/10.3389/fgene.2018.00410
- 584 Logue, M.W. *et al.* (2011) A Comprehensive Genetic Association Study of Alzheimer Disease in African
585 Americans, *Arch Neurol*, 68(12), 1569–1579. doi.org/10.1001/archneurol.2011.646
- 586 Mancuso, R. *et al.* (2022) Editorial: Infection, inflammation, and neurodegeneration: A critical path to
587 Alzheimer’s disease, Volume II, *Front Aging Neurosci*, 14:1044047. doi.org/10.3389/fnagi.2022.1044047
- 588 Mizutani, K. *et al.* (2022) Nectin-2 in general and in the brain, *Mol Cell Biochem*, 477(1), 167–180.
589 doi.org/10.1007/s11010-021-04241-y
- 590 Moore, K.B.E., Hung, T.J. and Fortin, J.S. (2023) Hyperphosphorylated tau (p-tau) and drug discovery in the
591 context of Alzheimer’s disease and related tauopathies, *Drug Discov Today*, 28(3):103487.
592 doi.org/10.1016/j.drudis.2023.103487
- 593 Moscoso, A. *et al.* (2021) ‘Longitudinal Associations of Blood Phosphorylated Tau181 and Neurofilament
594 Light Chain With Neurodegeneration in Alzheimer Disease’, *JAMA Neurol*, 78(4), 396–406. doi:
595 10.1001/jamaneurol.2020.4986

- 596 Nguyen, T.Q., Schmid, I. and Stuart, E.A. (2020) Clarifying causal mediation analysis for the applied
597 researcher: Defining effects based on what we want to learn HHS Public Access, *Psychol Methods*, 16,
598 10.1037/met0000299. doi.org/10.1037/met0000299
- 599 Nuovo, G.J. *et al.* (2022) The amplification of CNS damage in Alzheimer's disease due to SARS-CoV2
600 infection, *Ann Diagn Pathol*, 61:152057. doi.org/10.1016/j.anndiagpath.2022.152057
- 601 Ogawa, H. *et al.* (2022) Nectin-2 Acts as a Viral Entry Mediated Molecule That Binds to Human Herpesvirus
602 6B Glycoprotein B, *Viruses*, 14(1):160. doi.org/10.3390/v14010160
- 603 Oyekale, A.S. (2021) Willingness to Take Covid-19 Vaccines in Ethiopia: An Instrumental Variable Probit
604 Approach, *Int J Environ Res Public Health*, 18(17):8892. doi.org/10.3390/ijerph18178892
- 605 Pearl, J. (2014) Interpretation and Identification of Causal Mediation, *Psychological Methods*, 19(4), 459–481.
606 doi.org/10.1037/a0036434
- 607 Piekut, T. *et al.* (2022) Infectious agents and Alzheimer's disease, *J Integr Neurosci.*, 21(2):
608 73.doi.org/10.31083/j.jin2102073
- 609 Popov, V.A. *et al.* (2024) Prior infections are associated with smaller hippocampal volume in older women,
610 *Front Dement*, 3(2024). doi.org/10.3389/frdem.2024.1297193
- 611 Powell-Doherty, R.D. *et al.* (2020) Amyloid- β and p-Tau Anti-Threat Response to Herpes Simplex Virus 1
612 Infection in Primary Adult Murine Hippocampal Neurons, *J Virol*, 94(9), e01874-19.
613 doi.org/10.1128/jvi.01874-19
- 614 Purcell, S. and Chang, C. (2023). *PLINK 1.9*. <https://www.cog-genomics.org/plink/1.9/> [Accessed April 4,
615 2023].
- 616 Rajendrakumar, A. L., Arbeev, K. G., Bagley, O., Yashin, A. I., Ukraintseva, S., (2024). The SNP rs6859 in
617 NECTIN2 gene is associated with underlying heterogeneous trajectories of cognitive changes in older adults.
618 *BMC Neurol*, 24(1), 78. doi: 10.1186/s12883-024-03577-4
- 619 Ramos Bernardes da Silva Filho, S. *et al.* (2017) Neuro-degeneration profile of Alzheimer's patients: A brain
620 morphometry study, *NeuroImage Clin*, 15, 15–24. doi.org/10.1016/j.nicl.2017.04.001
- 621 R Core Team (2021) *R: A language and environment for statistical computing*. R Foundation for Statistical
622 Computing, Vienna, Austria. Available at: <https://www.R-project.org/> (Accessed: 15 May 2023).
- 623 Readhead, B. *et al.* (2018) Multiscale Analysis of Independent Alzheimer's Cohorts Finds Disruption of
624 Molecular, Genetic, and Clinical Networks by Human Herpesvirus, *Neuron*, 99(1), 64-82.
625 doi.org/10.1016/j.neuron.2018.05.023
- 626 Rijnhart, J.J.M. *et al.* (2021) Mediation analysis methods used in observational research: a scoping review and
627 recommendations', *BMC Med Res Methodol*, 21(226). doi.org/10.1186/S12874-021-01426-3
- 628 Sait, A. *et al.* (2021) Viral Involvement in Alzheimer's Disease, *ACS Chem Neurosci*, 12(7), 1049–1060.
629 doi.org/10.1021/acchemneuro.0c00719
- 630 Salvadó, G. *et al.* (2024) 'Disease staging of Alzheimer's disease using a CSF-based biomarker model', *Nat*
631 *Aging*, 4(5), 694–708. doi.org/10.1038/s43587-024-00599-y
- 632 Sathler, M.F. *et al.* (2022) HIV and FIV glycoproteins increase cellular tau pathology via cGMP-dependent
633 kinase II activation, *J Cell Sci*, 135(12): jcs259764. doi.org/10.1242/jcs.259764
- 634 Shaw, L.M. *et al.* (2009) Cerebrospinal fluid biomarker signature in Alzheimer's disease neuroimaging
635 initiative subjects, *Annals of Neurology*, 65(4), 403–413. doi.org/10.1002/ana.21610
- 636 Shen, W.-B. *et al.* (2022) SARS-CoV-2 invades cognitive centers of the brain and induces Alzheimer's-like
637 neuropathology, *bioRxiv: [Preprint]*, (2022.01.31.478476). doi.org/10.1101/2022.01.31.478476

- 638 Suárez-Calvet, M. *et al.* (2020) ‘Novel tau biomarkers phosphorylated at T181, T217 or T231 rise in the initial
639 stages of the preclinical Alzheimer’s continuum when only subtle changes in A β pathology are detected’,
640 *EMBO Mol Med*, 12(12), e12921. doi: 10.15252/emmm.202012921
- 641 Tang, Z. *et al.* (2022) Treponema denticola Induces Alzheimer-Like Tau Hyperphosphorylation by Activating
642 Hippocampal Neuroinflammation in Mice, *J Dent Res*, 101(8), 992–1001.
643 doi.org/10.1177/00220345221076772
- 644 Thijssen, E.H. *et al.* (2020) ‘Diagnostic value of plasma phosphorylated tau181 in Alzheimer’s disease and
645 frontotemporal lobar degeneration’, *Nat Med*, 26(3), 387–397. doi: 10.1038/s41591-020-0762-2
- 646 Thijssen, E.H. *et al.* (2021) ‘Plasma phosphorylated tau 217 and phosphorylated tau 181 as biomarkers in
647 Alzheimer’s disease and frontotemporal lobar degeneration: a retrospective diagnostic performance study’,
648 *Lancet Neurol*, 20(9), 739–752.
- 649 Tingley, D. *et al.* (2014) mediation: R package for causal mediation analysis, *Journal of Statistical Software*, 59
650 (5), 1–38. doi.org/10.18637/jss.v059.i05
- 651 Ukraintseva, S. *et al.* (2023) Vaccination Against Pneumonia May Provide Genotype-Specific Protection
652 Against Alzheimer’s Disease, *J Alzheimers Dis.*, 96(2), 499–505. doi.org/10.3233/jad-230088
- 653 Vacchiano, V. *et al.* (2023) ‘Elevated plasma p-tau181 levels unrelated to Alzheimer’s disease pathology in
654 amyotrophic lateral sclerosis’, *J Neurosurg Psychiatry*, 94(6), pp. 428–435. doi: 10.1136/jnnp-2022-330709
- 655 Wagenmakers, E.-J. and Farrell, S. (2004) AIC model selection using Akaike weights, *Psychonomic Bulletin &*
656 *Review*, 11(1), 192–196. doi.org/10.3758/bf03206482
- 657 Weiner, M.W. *et al.* (2010) The Alzheimer’s Disease Neuroimaging Initiative: Progress report and future plans,
658 *Alzheimer’s & Dementia*, 6(3), 202–211. doi.org/10.1016/j.jalz.2010.03.007
- 659 Weiner, M.W. *et al.* (2017) The Alzheimer’s Disease Neuroimaging Initiative 3: Continued innovation for
660 clinical trial improvement, *Alzheimer’s & Dementia*, 13(5), 561–571.
661 doi.org/10.1016/j.jalz.2016.10.006
- Wennström, M. *et al.* (2024) ‘The Relationship between p-tau217, p-tau231,
662 and p-tau205 in the Human Brain Is Affected by the Cellular Environment and Alzheimer’s Disease Pathology’,
663 *Cells*, 13(4), 331. doi: 10.3390/cells13040331
- 664 Wickham, H. (2016) *ggplot2: Elegant Graphics for Data Analysis Using the Grammar of Graphics*. Springer-
665 Verlag New York. ISBN 978-3-319-24277-4. <https://ggplot2.tidyverse.org>
- 666 Williams, R. (2012) ‘Using the margins command to estimate and interpret adjusted predictions and marginal
667 effects’, *The Stata Journal*, 12(2), 308–331. doi.org/10.1177/1536867x1201200209
- 668 Xiao, Q. *et al.* (2022) The Relationship Between Low-Density Lipoprotein Cholesterol and Progression of Mild
669 Cognitive Impairment: The Influence of rs6859 in PVRL2, *Front. Genet.*, 13.
670 doi.org/10.3389/fgene.2022.823406
- 671 Yashin, A.I. *et al.* (2018) Hidden heterogeneity in Alzheimer’s disease: Insights from genetic association
672 studies and other analyses, *Exp Gerontol.* 107, 148–160. doi.org/10.1016/j.exger.2017.10.020
- 673 Yin, M. *et al.* (2016) Probit Models to Investigate Prevalence of Total Diagnosed and Undiagnosed Diabetes
674 among Aged 45 Years or Older Adults in China, *PLoS ONE*, 11(10): e0164481.
675 doi.org/10.1371/journal.pone.0164481
- 676 Yong, S.J. *et al.* (2021) The Hippocampal Vulnerability to Herpes Simplex Virus Type I Infection: Relevance
677 to Alzheimer’s Disease and Memory Impairment, *Front Cell Neurosci*, 15:695738.
678 doi.org/10.3389/fncel.2021.695738
- 679 Yu, L. *et al.* (2023) ‘Plasma p-tau181 and p-tau217 in discriminating PART, AD and other key
680 neuropathologies in older adults’, *Acta Neuropathol*, 146(1), 1–11. doi: 10.1007/s00401-023-02570-4.
- 681 Zetterberg, H. (2017) ‘Review: Tau in biofluids – relation to pathology, imaging and clinical features’,
682 *NeuropatholAppl Neurobiol*, 43(3), 194–199. doi: 10.1111/nan.12378.

683 Zetterberg, H. and Blennow, K. (2021) ‘Moving fluid biomarkers for Alzheimer’s disease from research tools
684 to routine clinical diagnostics’, *Mol Neurodegener*, 16(1),10. doi: 10.1186/s13024-021-00430-x

685 Zhang, Z. *et al.* (2016) Causal mediation analysis in the context of clinical research, *Annals of Translational*
686 *Medicine*, 4(21):425. doi.org/10.21037/atm.2016.11.11

687

688 **Corresponding Author information**

689 *Correspondence to ALR and SU, Email address: alr75@duke.edu, Svetlana.Ukrainitseva@duke.edu

690

691

692